Photochemical & Photobiological Sciences (2021) 20:321–326
https://doi.org/10.1007/s43630-021-00011-3

TECHNICAL NOTES

Exploiting the photoactivity of bacterial reaction center to investigate liposome dynamics

Emiliano Altamura[1] · Francesco Milano[2] · Pasquale Stano[3] · Fabio Mavelli[1]

Received: 10 December 2020 / Accepted: 8 January 2021 / Published online: 10 February 2021

Abstract
Charge recombination kinetics of bacterial photosynthetic protein Reaction Center displays an exquisite sensitivity to the actual occupancy of ubiquinone-10 in its Q_B-binding site. Here, we have exploited such phenomenon for assessing the growth and the aggregation/fusion of phosphocholine vesicles embedding RC in their membrane, when treated with sodium oleate.

1 Introduction

Besides their well-known use in biophysics, biochemistry and medicine, in recent years, artificial lipid vesicles (liposomes) have attracted attention as whole-cell models in "bottom-up" synthetic biology [1–4]. The resulting structures, when hierarchically organized in more complex systems called "artificial cells", "synthetic cells" or "protocells", serve as cellular models to understand fundamental principles of life or to develop frontier biotechnological applications.

One interesting direction refers to dynamical morphological transformations deriving from vesicle–vesicle or vesicle–amphiphile interactions, such as: amphiphile uptake, membrane growth, division, fusion, shape changes, etc. Such processes reveal how artificial cells can accomplish several transformations in the absence of complex macromolecular machineries [4–6]. For example, fatty acid vesicles can grow-and-divide if stimulated by the addition of a proper fatty acid precursor (e.g., fatty acid anhydride) [7]. The interaction between vesicles made of phospholipids and those made of fatty acids also gives rise to an interesting dynamics, based on molecular transfer of vesicle constituents from one population to the other [8]. As a third example, the presence of fatty acids in PC membranes has made possible a spontaneous vesicle division driven by an encapsulated enzyme reaction, which triggers the division by an intravesicle pH change [9].

The photosynthetic Reaction Center (RC), a photoresponsive transmembrane protein, is a widely used model system to investigate the transduction of light into chemical energy [10–12]. RC can be reconstituted in vesicles to mimic the physiological transmembrane conditions. In particular, a single white light flash induces a charge separation within the RC-bound cofactors, based on electron transfer of one electron from the bacteriochlorophyll special pair (D) to the acceptor quinone molecules (Q) located in the Q_A-site (tightly bound) or in the Q_B-site (loosely bound). The charge-separated states ($D^+Q_A^-$ or $D^+Q_AQ_B^-$) recombine to the initial state by an internal charge recombination (c. r.) (Fig. 1a). The kinetics of the c. r. reaction depends upon the occupancy of the Q_B-site [13]. In turn, this depends on the concentration and diffusion of unbound Q, which—if hydrophobic, as in the case of ubiquinone-10 natively present in the RC and employed in the present study—also resides in the liposome membrane or in other available hydrophobic domains (the mechanisms of charge separation and recombination is illustrated in Figure S1).

✉ Fabio Mavelli
fabio.mavelli@uniba.it

Emiliano Altamura
emiliano.altamura@uniba.it

Francesco Milano
Francesco.milano@cnr.it

Pasquale Stano
pasquale.stano@unisalento.it

[1] Department of Chemistry, Università Degli Studi Di Bari "Aldo Moro", Via Orabona 4, 70125 Bari, Italy

[2] Institute of Science of Food Production (ISPA), CNR, Str. Provinciale Lecce-Monteroni, 73100 Lecce, Italy

[3] Department of Biological and Environmental Sciences and Technologies (DiSTeBA), University of Salento, Str. Provinciale Lecce-Monteroni, 73100 Lecce, Italy

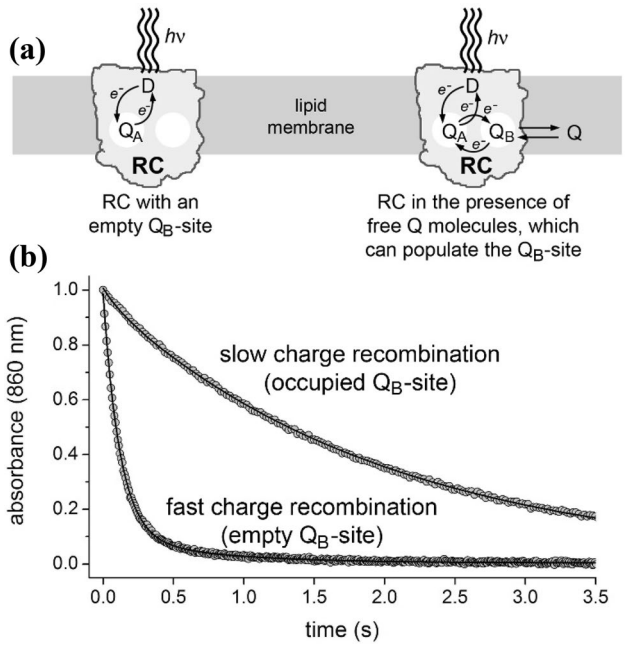

Fig. 1 **a** Photoinduced electron transfer reactions and charge recombination in photosynthetic RC in absence (left) and presence (right) of exogenous quinone. **b** Recorded traces of the charge recombination reaction for the above-depicted cases

The fine-tuned dependence of the c.r. kinetics upon the occupancy of the Q_B-site offers the opportunity to probe the "environmental" state around the RC, providing information on the processes within the vesicle membrane [14], including membrane growth, vesicle fusion or aggregation, uptake of amphiphiles, etc.

In this paper, we present an investigation on the use of the kinetics of the charge recombination reactions measured via transient absorbance spectroscopy, for assessing dynamical processes of phosphatidylcholine vesicles triggered by sodium oleate. Traditionally, this kind of studies on the dynamics of morphological change of vesicle membranes are performed by direct inspection (electron microscopy and light microscopy), by monitoring the size changes (light scattering, turbidimetry), or by monitoring the fate of the solutes entrapped in the vesicle lumen or in their membrane (often via fluorescence) [15]. On the other hand, monitoring of lipid vesicle transformations by following the change of a transmembrane protein activity is only one aspect of our study. At the same time, we aim to show that the Reaction Center keeps its functionality during vesicle morphology changes (membrane growth due to the uptake of fresh fatty acid molecules), and during membrane solute exchange due to vesicle–vesicle interactions.

2 Materials and methods

2.1 Materials

The photosynthetic Reaction Centers were extracted and purified from *R. sphaeroides* (strain R-26) [16] using a buffer containing 20 mM Tris–HCl, LDAO (lauryl dimethyl N-Oxide, 0.03% wt./vol) and 1 mM EDTA at pH 8.0. In this preparation, the Q_{total}:RC molar ratio was 1.8 ± 0.05. When needed, the Q molecules still bound to the Q_B-site were removed according to Okamura et al. [17], obtaining Q_B-depleted RC, whose Q_{total}:RC molar ratio was 1.05 ± 0.05. When full Q_B occupation was required, excess quinone was added to the system.

2.2 Vesicle preparation

Small unilamellar vesicles of soybean phosphatidylcholine (PC from Sigma-Aldrich), containing RC or ubiquinone-10 (UQ_{10}, here indicated as Q) or both were prepared by the micelle-to-vesicle transition method, as described in Milano et al. [18], and briefly explained in SI. We prepared the following types of vesicles: (a) DQ_A@PC with PC:RC molar ratio of 8000:1; (b) DQ_AQ_B@PC with PC:RC molar ratio of 8000:1 and Q_B-site 80% occupied, indicated by a symbol in smaller size; (c) DQ_AQ_B@PC with PC:RC:Q molar ratio of 8000:1:32 and Q_B-site fully occupied; (d) Q@PC with PC:Q molar ratio of 8000:32. Actual concentration values are given in table S1. All experiments were carried out in 50 mM K–phosphate/100 mM KCl buffer (pH 6.9). The method used for RC reconstitution does not allow for precise control of the protein orientation, therefore the proteins could plausibly be oriented 50% outward and 50% inward of the vesicles.

2.3 Sodium oleate addition

Sodium oleate (OL) was added from an 80 mM stock solution in Milli-Q water in which OL is present as micellar aggregates (OLm).

2.4 Charge recombination measurements and data analysis

In all experiments, the c.r. kinetics was recorded at 25 °C up to complete decay by means of a custom designed spectrophotometer (Figure S2). The decay curves, after normalization to $A(0) = 1$, were fitted to a bi-exponential decay function, to keep into account the simultaneously occurring charge recombination paths, namely the fast one (f: $D^+Q_A^- \rightarrow DQ_A$) and the slow one (s: $D^+Q_AQ_B^- \rightarrow DQ_AQ_B$), Eq. 1:

$$A(t) = A_f e^{-k_f t} + A_s e^{-k_s t}, \quad (1)$$

A_f and A_s being the amplitudes of the fast and the slow decay components, respectively, whereas k_f and k_s are the corresponding rate constants. Recalling that $A_f + A_s = 1$, and fixing $k_f = 9.0\ s^{-1}$ [19], experimental points were fitted by varying A_s and k_s, both depending on the Q_B-site occupancy [13, 20, 21]. The area under the curve (S) of the bi-exponential function has been calculated accordingly. S has the following analytical expression (Eq. 2):

$$S = \int_0^\infty A(t)dt = \frac{1}{k_f} + A_s\left(\frac{1}{k_s} - \frac{1}{k_f}\right), \quad (2)$$

and ranges from $1/k_f = 0.11$ s (when $A_s \to 0$) to $1/k_s$ when the slow decay dominates (i.e., $A_s \to 1$), in presence of an excess of added quinones. For RC in PC liposomes treated with oleate, the value of k_s is 0.42 s^{-1}, and thus $S \to 2.38$ s. The range of existence of S (0.11 to 2.38 s) allows monitoring the Q_B-site occupancy.

A parameter p correlated to the Q_B-occupancy, according to (Eq. 3):

$$p = \frac{S - 0.11}{2.38 - 0.11}, \quad (3)$$

ranges between 0 (in Q_B-depleted RCs) and 1 (when the Q_B-site is fully occupied). The reported p values in replicate experiments vary of about ± 10%, but despite the numerical variations, the observed trends were maintained.

2.5 Dynamic light scattering

Vesicles diameters (z-averages) were measured by dynamic light scattering (DLS, Zetasizer Nano).

3 Results and discussion

We carried out kinetic assays of vesicle systems according to three different experimental designs schematically depicted in Fig. 2a.

3.1 Type I experiments

3.1.1 Type Ia

DQ_AQ_B@PC samples were treated with OLm (OL:PC = 1) and the c.r. kinetics was recorded after different time intervals. At each time point, p was calculated from the fitting parameters and Fig. 2b shows the variation of p over time. In particular, p suddenly decreases from 0.28 to 0.15 soon after the mixing, with minor changes at longer time. At 45 min, p reaches a stable value of 0.17.

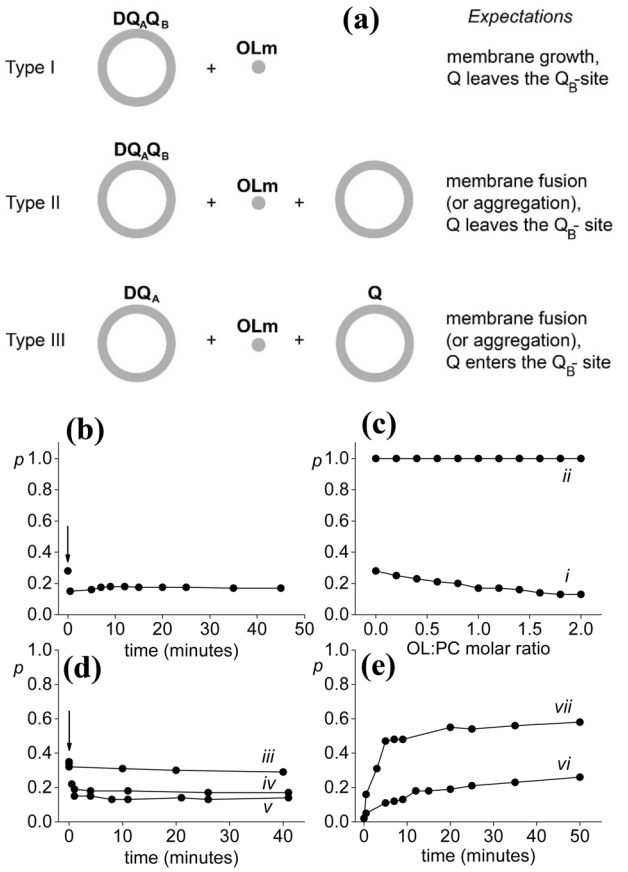

Fig. 2 **a** Schematic representation of the three types of experiments. **b** Type Ia experiments. **c** Type Ib experiments (curve i). Type Ic experiment (curve ii); **d** type II experiments. **e** Type III experiments. Note: p values should be considered ± 10% (see text for details)

3.1.2 Type Ib

DQ_AQ_B@PC vesicles were treated with increasing amounts of OLm to scan the OL:PC molar ratio from 0 to 2. Data are shown in Fig. 2c (curve i) with a monotone decrease of p from 0.28 to 0.13.

3.1.3 Type Ic

An experiment similar to Type Ib was performed with DQ_AQ_B@PC samples and data are shown in Fig. 2c (curve ii). In this case, due to the addition of an excess of free quinones (RC:Q is equal to 1:32), the recombination kinetics is always mono-exponential. As result, the value of p is always close to 1 (see SI for further details). The constant k_s slightly slows down due to the insertion of an increasing amount of negative charges inside the vesicle bilayer because of the

uptake of OL. Indeed, around 3% of oleic acid molecule are deprotonated on the lipid bilayer at pH = 6.9 (p*K*a = 8.4).

3.2 Type II experiments

DQ_AQ_B@PC vesicles were mixed with an equal amount of pure PC vesicles, with or without the pre-treatment of each vesicle sample with OL (OL:PC = 1 for DQ_AQ_B@PC, and OL:PC = 2 for pure vesicles). Curve iii of Fig. 2d refers to mixing of DQ_AQ_B@PC with pure PC vesicles. Substantially, no changes in *p* value was recorded. Curves iv and v of Fig. 2d refer to mixing of DQ_AQ_B@PC with pure PC vesicles in presence of oleate under stirring and unstirring conditions, respectively. In both cases, *p* halves in comparison to curve iii.

3.3 Type III experiments

DQ_A@PC and *Q*@PC vesicles were separately pre-treated with OL, then mixed together (1:1 v/v) to a final *Q*:RC molar ratio of 32. Curves vi and vii of Fig. 2e refer to experiments carried out by adding different amounts of OL to DQ_A@PC vesicles, i.e., OL:PC = 1 (curve vi) and 2 (curve vii). *Q*@PC vesicles, instead, have been always pre-treated with 2 equivalents of OL. The experiments clearly show that *Q* molecules rapidly populate the RC Q_B-site, and *p* rapidly increases from 0 to 0.26 (at low OL content, curve vi) or to 0.56 (at high OL content, curve vii).

4 Discussion

The outcome of the experimental setup shows that monitoring the *S* value in liposome-reconstituted RCs is a convenient method for assessing vesicle transformations of the types described in this study (interaction with amphiphiles/surfactants, vesicle growth, aggregation, solute exchange, etc.). The well-known OL micelles interaction with PC vesicles [22, 23] represents a suitable study case to illustrate our claim.

In water, sodium oleate (OL) is present as self-assembled micelles in equilibrium with OL monomers. The pH of the micellar solution self-establishes around 10.5. When added to aqueous solution at lower pH, OL molecules become protonated and slowly self-convert to other association forms (e.g., vesicles at pH 8–9), but below pH 7 long chain fatty acids start becoming water insoluble [24–26]. In presence of PC vesicles, the added OL molecules quickly insert in the PC membrane [27–29], leading to the increase of vesicle surface (vesicle growth) [23], changing of membrane properties (e.g., fluidity increases) [8], and endowing the resulting mixed PC/OL membranes with a negative charge. While at pH 8.5, a plain PC vesicle growth has been reported [23], at lower pH (e.g., 7.4) vesicle growth can also lead to vesicle aggregation/fusion and other complex transformations[1] [30]. In this study, the OL addition to PC vesicles has been investigated at pH 6.9 (phosphate buffer). This pH was chosen since in these conditions, while RC still maintains its functionality, a higher fraction of the protonated OL molecules in the PC bilayer makes the resulting mixed OL/PC vesicles more prone to vesicle–vesicle interactions and solute exchange. Accordingly, when OL molecules are rapidly absorbed by the PC membranes, they determine vesicle growth, the observed dilution effect of quinones, and the higher flexibility of mixed PC/OL membrane. Thus, a complex scenario takes place, where both vesicle growth and vesicle fusion/aggregation can coexist. Moreover, it is important to stress that since our method is sensitive only to the perturbation of the membrane size and composition, it cannot be used to prove vesicle–vesicle fusion (whereby the mixing of the internal aqueous solutes occurs). Despite this complexity, whose details are outside the purpose of the publication, the *S* analysis of RC c.r. kinetics, accompanied by a simple DLS size determination, leads to quite straightforward conclusions about the occupancy of the RC Q_B-site, and thus, indirectly, about the dominant vesicle transformation.

Let us discuss how experimental *S* and *p* values can be used to decipher vesicle transformations. The OL insertion in PC membranes leads to an increase of the membrane surface, diluting both RC and Q. Consequently, by the law of mass action, the binding of *Q* to RC becomes less favored and *p* decreases. However, since the membrane fluidity increases, we expect that the interaction between RC and *Q* becomes kinetically favored.

The RC c.r. kinetics also helps for detecting vesicle fusion/aggregation in two complementary approaches. It is expected that mixing DQ_AQ_B@PC with plain PC vesicles will lead to dilution of RC and *Q* on a larger hydrophobic surface (*p* decreases). In contrary, mixing DQ_A@PC with Q@PC will lead to the encounter of initially separated RC and *Q*, with a clear-cut increase of *p*.[2]

In type I experiments, OLm was added to DQ_AQ_B@PC vesicles. OL adsorption is rapid [27–29] and the negligible changes in the c. r. kinetics observed in time confirm essentially that all OL micelles were uptaken soon after the addition [22, 23] (Fig. 2b). In the case of OL:PC = 1, DLS reveals that the vesicle diameter increases from 42 ± 6

[1] Aggregation and fusion can happen because of the propensity of oleic acid molecules, formed by OL protonation, to self-assemble as non-lamellar inverted hexagonal structures, which can be fusogenic. At even lower pH, oleic acid separates as oil droplets [30].

[2] In principle, in addition to fusion and aggregation, RC and/or *Q* could be shuttled between different vesicles by hydrophobic oleic acid/oleate-based carriers.

to 51 ± 5 nm ($n = 3$ independent experiments), compatible with ~ 100% insertion of OL in the PC vesicle membrane. Because p decreases, we conclude that the dilution of RC and Q over a larger hydrophobic surface is the dominant effect. A similar pattern is observed when the OL:PC molar ratio is varied from 0 to 2 (Fig. 2c, curve i). Expectedly, at high OL:PC, a larger p decrease is measured, because of the larger amount of added hydrophobic surface. Note, however, that these first set of experiments has been carried out with Q:RC = 0.8, which is a condition whereby the dilution of RC and Q is expected to be especially effective to remove Q from the Q_B-site. In contrary, if Q:RC = 32, the dilution effect (reduction of p) is overtaken by the mass action effect that keeps p value always very close to one. (Fig. 2c, curve ii). We conclude that OL insertion into PC membrane carried out at different Q:RC ratios shows effects that are visible only when the Q_B-site in not fully saturated.

In type II experiments (Fig. 2d), DQ_AQ_B@PC vesicles are mixed with pure PC vesicles possibly pre-treated with OLm to favor the inter-vesicles interactions. At lower pH, vesicle fusion/aggregation is expected, as mentioned above [22, 23]. In type II experiments (as well as in type III one), DLS supports vesicle fusion/aggregation but does not allow distinction between the two mechanisms. The average vesicle diameter changed from 53 ± 8 (OLm-treated vesicles) to 80 ± 10 nm ($n = 2$) after the two populations are mixed.

PC vesicles not treated with OL do not show a significant change neither in the diameters (from 38 ± 3 to 38 ± 2 nm, $n = 2$) nor in the c. r. curve (p ~ constant, Fig. 2d, curve iii). This confirms that PC vesicles are stable and no significant transfer of RC and/or Q occurs spontaneously between the two vesicle populations that would lead to a reduction of p. In contrast, when DQ_AQ_B@PC vesicles and pure PC vesicles are pre-treated with OLm (OL:PC = 1 and 2, respectively), a clear reduction of p is observed immediately after mixing (Fig. 2d, curves iv and v). The time profiles after mixing indicate that the vesicle fusion/aggregation occurs rapidly after the mixing. Moreover, the process is not affected by stirring. Under these experimental conditions (Q:RC = 0.8), it is expected that following the OL-induced fusion/aggregation, Q and RC are diluted in a larger hydrophobic surface, leading to a reduction of p, as in the case of Fig. 2b and c curve i.

In type III experiments, DQ_A@PC vesicles are mixed with Q@PC vesicles (final Q:RC = 32). Here, the RC is initially deprived of Q (p ~ 0) and the experiments aim at measuring how well RC and Q mix. As in type II experiments, we expect vesicle fusion/aggregation, but this time with a consequent increase of p because the slow phase of c. r. becomes accessible only when Q binds to the RC Q_B-site. The curves of Fig. 2e show that Q and RC mix with a rate that depends on the OL amount, confirming that OL specifically determines the abovementioned mechanism. The OL amount tunes both the extent of mixing (final p ~ 0.26 or 0.56) and the rate of mixing (k_{oss} ~ 0.059 or 0.160 min^{-1}), depending on its amount (OL:PC = 1 or 2, respectively).

5 Concluding remarks

Here, we have shown a novel experimental method that allows monitoring vesicle transformation based on the occupancy of the Q_B-site of the photosynthetic Reaction Center. From the c.r. kinetics of the RC, it is possible to extract an operative parameter p that can be used to indirectly assesses the state of the vesicle membrane where exogenous Q is located. Despite our method requires a specially designed kinetic spectrophotometer, we claim that the simple S-approach is sufficient for monitoring vesicle transformations, although in-depth analysis of individual variations of k_s and A_s would shed more light on mechanistic details of the RC activity.

We have discussed the well-known case whereby OL micelles are added to PC vesicles, explaining how the variations of p can be interpreted on the basis of known molecular and supramolecular mechanisms. Moreover, our novel approach clearly evidences that the Reaction Center keeps its photoactivity during the membrane morphology changes. Therefore, in a near future, this method could be applied to investigations of other phenomena, such as lipid synthesis in artificial cells driven by light energy that might induce lipid compartment division. Clearly, additional complementary techniques such as fluorescence, DLS, zeta-potential, and electron microscopy are necessary to fully elucidate the mechanism under enquiry.

Supplementary Information The online version contains supplementary material available at https://doi.org/10.1007/s43630-021-00011-3.

Acknowledgements The authors are grateful to Massimo Trotta (Institute for Physical and Chemical Processes, CNR-Bari, Italy) for helpful discussions.

Compliance with ethical standards

Conflict of interest The authors declare that they have no conflicts of interest relevant to the manuscript submitted to Photochemical and Photobiological Sciences.

References

1. Luisi, P. L., Ferri, F., & Stano, P. (2006). Approaches to semi-synthetic minimal cells: A review. *Naturwissenschaften, 93,* 1–3.
2. Shin, J., & Noireaux, V. (2012). An *E.coli* cell-free expression toolbox: Application to synthetic gene circuits and artificial cells. *ACS Synthetic Biology, 1,* 29–41.

3. Salehi-Reyhani, A., Ces, O., & Elani, Y. (2017). Artificial cell mimics as simplified models for the study of cell biology. *Experimental Biology and Medicine., 242,* 1309–1317.
4. Schwille, P., Spatz, J., Landfester, K., Bodenschatz, E., Herminghaus, S., Sourjik, V., et al. (2018). Sundmacher MaxSynBio: avenues towards creating cells from the bottom up. *Angewandte Chemie International Edition., 57,* 13382–13392.
5. Budin, I., & Szostak, J. W. (2010). Expanding roles for diverse physical phenomena during the origin of life. *Annual Review of Biophysics*, *39*, 245–263.
6. Hardy, M. D., Yang, J., Selimkhanov, J., Cole, C. M., Tsimring, L. S., & Devaraj, N. K. (2015). Self-reproducing catalyst drives repeated phospholipid synthesis and membrane growth. *Proceedings of the National Academy of Sciences, 112,* 8187–8192.
7. Walde, P., Wick, R., Fresta, M., Mangone, A., & Luisi, P. L. (1994). Autopoietic self-reproduction of fatty acid vesicles. *Journal of the American Chemical Society., 116,* 11649–11654.
8. Budin, I., & Szostak, J. W. (2011). Physical effects underlying the transition from primitive to modern cell membranes. *Proceedings of the National Academy of Sciences, 108,* 5249–5254.
9. Miele, Y., Medveczky, Z., Holló, G., Tegze, B., Derényi, I., Hórvölgyi, Z., et al. (2020). Self-division of giant vesicles driven by an internal enzymatic reaction. *Chemical Science, 11,* 3228–3235.
10. Milano, F., Agostiano, A., Mavelli, F., & Trotta, M. (2003). Kinetics of the quinone binding reaction at the QB site of reaction centers from the purple bacteria *Rhodobactersphaeroides* reconstituted in liposomes. *European Journal OF Biochemistry, 270,* 4595–4605.
11. Tangorra, R. R., Operamolla, A., Milano, F., Omar, O. H., Henrard, J., Comparelli, R., et al. (2015). Assembly of a photosynthetic reaction center with ABA tri-block polymersomes: Highlights on protein localization. *Photochemical & Photobiological Sciences, 14,* 1844–1852.
12. Altamura, E., Milano, F., Tangorra, R. R., Trotta, M., Omar, O. H., Stano, P., & Mavelli, F. (2017). Highly oriented photosynthetic reaction centers generate a proton gradient in synthetic protocells. *Proceedings of the National Academy of Sciences United State of America, 114,* 3837–3842.
13. Mavelli, F., Trotta, M., Ciriaco, F., Agostiano, A., Giotta, L., Italiano, F., et al. (2014). The binding of quinone to the photosynthetic reaction centers: kinetics and thermodynamics of reactions occurring at the QB-site in zwitterionic and anionic liposomes. *European Biophysics Journal*, *43*, 301–315.
14. Trotta, M., Agostiano, A., Milano, F., & Nagy, L. (2002). Response of membrane protein to the environment: the case of photosynthetic Reaction Centre. *Materials science & engineering C*, *22*, 263–267.
15. Kundu, N., Mondal, D., & Sarkar, N. (2020). Dynamics of the vesicles composed of fatty acids and other amphiphile mixtures: Unveiling the role of fatty acids as a model protocell membrane. *Biophysical Reviews, 12,* 1117–1131.
16. Isaacson, R. A., Lendzian, F., Abresch, E. C., Lubitz, W., & Feher, G. (1995). Electronic structure of QA in reaction centers from *Rhodobactersphaeroides*. I. Electron paramagnetic resonance in single crystals. *Biophysical Journal, 69,* 311–322.
17. Okamura, M. Y., Isaacson, R. A., & Feher, G. (1975). Primary acceptor in bacterial photosynthesis: Obligatory role of ubiquinone in photoactive reaction centers of *Rhodopseudomonasspheroides*. *Proceedings of the National Academy of Sciences, 72,* 3491–3495.
18. Milano, F., Italiano, F., Agostiano, A., & Trotta, M. (2009). Characterisation of RC-proteoliposomes at different RC/lipid ratios. *Photosynthesis Research, 100,* 107–112.
19. Milano, F., Tangorra, R. A., Hassan Omar, O., Ragni, R., Operamolla, A., Agostiano, A., Farinola, G. M. & Trotta, M. (2012). *Angewandte Chemie International Edition English, vol. 51*, pp. 11019–11023.
20. Shinkarev, V. P., & Wraight, C. A. (1997). The interaction of quinone and detergent with reaction centers of purple bacteria. I. Slow quinone exchange between reaction center micelles and pure detergent micelles. *Biophysical Journal, 72,* 2304–2319.
21. Altamura, E., Albanese, P., Stano, P., Trotta, M., Milano, F., & Mavelli, F. (2020). Charge recombination kinetics of bacterial photosynthetic reaction centres reconstituted in liposomes: Deterministic versus stochastic approach. *Data, 5,* 53.
22. Blöchliger, E., Blocher, M., Walde, P., & Luisi, P. L. (1998). Matrix effect in the size distribution of fatty acid vesicles. *The Journal of Physical Chemistry B., 102,* 10383–10390.
23. Chen, I. A., & Szostak, J. W. (2004). A kinetic study of the growth of fatty acid vesicles. *Biophysical Journal, 87,* 988–998.
24. Gebicki, J. M., & Hicks, M. (1973). Ufasomes are stable particles surrounded by unsaturated fatty acid membranes. *Nature, 243,* 232–234.
25. Hargreaves, W. R., & Deamer, D. W. (1978). Liposomes from ionic, single-chain amphiphiles. *Biochemistry, 17,* 3759–3768.
26. Morigaki, K., & Walde, P. (2007). Fatty acid vesicles. *Current Opinion in Colloid & Interface Science, 12,* 75–80.
27. Storch, J., & Kleinfeld, A. M. (1986). Transfer of long-chain fluorescent free fatty acids between unilamellar vesicles. *Biochemistry, 25,* 1717–1726.
28. Simard, J. R., Kamp, F., & Hamilton, J. A. (2008). Measuring the adsorption of fatty acids to phospholipid vesicles by multiple fluorescence probes. *Biophysical Journal, 94,* 4493–4503.
29. Thomas, R. M., Baici, A., Werder, M., Schulthess, G., & Hauser, H. (2002). Kinetics and mechanism of long-chain fatty acid transport into phosphatidylcholine vesicles from various donor systems. *Biochemistry, 41,* 1591–1601.
30. Edwards, K., Silvander, M., & Karlsson, G. (1995). Aggregate structure in dilute aqueous dispersions of oleic acid/sodium oleate and oleic acid/sodium oleate/egg phosphatidylcholine. *Langmuir, 11,* 2429–2434.